Use of Calibration Maneuvers for Improved Performance of Strapdown Attitude Reference Systems

Kenneth R. Lorell*
NASA Ames Research Center, Moffett Field, Calif.

Conventional strapdown configurations require precise knowledge of the orientation of the gyro input axes as well as a moderately large, fast computer to provide inertial attitude. This paper presents the mechanization and discusses the operation and performance of an omnidirectional, strapdown pointing control system called All Sky Pointer which does not require precise gyro alignment or a sophisticated computer. Errors caused by gyro-optical sensor misalignment, gyro-integrator bias, and scale factor error are compensated for by the use of calibration maneuvers. Control and computation are provided by an electronics package utilizing technology similar to that found in hand-held calculators. Simulation results indicate that sub arc-minute pointing performance is possible and pointing errors are reduced by as much as an order of magnitude compared with uncompensated systems.

Nomenclature

A, A_{ij} = gyro alignment matrix and elements
A^*, A^*_{ij} = apparent alignment matrix and elements
b_{Gj}, B_{Ij} = gyro and integrator biases, respectively
B_j = gyro-integrator bias compensation
$K_{RI,2,3}$ = roll axis gyro output compensation terms
$K_{\gamma I,2,3}$ = yaw axis gyro output compensation terms
R_j = σ of the gyro-integrator noise
$S_{GI,2,3}$, $S_{I,1,2,3}$ = gyro and integrator scale factors, respectively
T = gyro-integrator drift observation period
Tcm = time required to perform a 360° calibration maneuver
$T_{PI,2}$ = time required to pitch to and from Canopus
$\gamma_{1,2,3}$ = angular error caused by rate noise
$\gamma_{R1,2,3}$ = angular error during roll calibration maneuver
$\gamma_{Y1.2.3}$ = angular error during yaw calibration maneuver
$\delta(t)$ = Kronecker delta
$\epsilon_{1,2,3}$ = drift compensation error
$\Theta_{R1,2,3}$ = angle measured at completion of roll calibration maneuver
$\Theta_{Y1,2,3}$ = angle measured at completion of yaw calibration maneuver
$\theta_{m1,2,3}$ = measured body angles
$\theta_{R1,2,3}$ = body angle measured during a roll maneuver
$\theta_{Y1,2,3}$ = body angle measured during a yaw maneuver
$\theta_{2,3c}$ = desired body angle in yaw and roll axes
σ = standard deviation
$\sigma_{Y,R}$ = standard deviation of error during yaw and roll maneuver
$\omega_{1,2,3}$ = body rates along principal axes
$\omega_{2,3c}$ = commanded body rate
$\hat{(\ )}$ = estimate
$E\{\ \}$ = expected value
$\dot{(\ )}$ = time derivative

Introduction

THE frequent and relatively inexpensive access to the orbital environment to be provided in the near future by the Space Shuttle has motivated a need for reliable, moderate performance pointing and stabilization systems. In the past, sub arc-minute pointing accuracy (suitable for many types of astronomical investigations[1-4]) could be obtained only through the use of a combination of complex and expensive components such as floated gyros, stable platforms, multiple, gimbaled star trackers and usually some type of flight or ground-based computer.[5,6] A simplified sysem would, ideally, depend on as few of these components as possible.

Strapdown pointing control systems are an attractive alternative concept because they eliminate the complicated electromechanical stable platform. Divergence of errors and the requirement for sophisticated computer hardware and software negates some of this advantage, however.[7] Improved performance has been obtained in a number of hybrid strapdown systems by augmenting the basic gyro information with the outputs from horizon, star or sun sensors. SPARS (Space Precision Attitude Reference System)[8] periodically updates the estimate of the vehicle's attitude with the signals from V-slit star sensors. Coffman[9] has designed a filter which estimates gyro bias and scale factor errors of a maneuvering system by comparing predicted star positions with sampled star tracker measurements. The Misalignment Estimation Software System[5] was developed to precisely estimate misalignments between the IRU and star tracker axes on the OAO spacecraft using a ground-based digital computer and remotely-commanded spacecraft maneuvers. All of these concepts require moderately fast general purpose digital computers in addition to at least one orbit period in order to reach steady state.

This paper reports a strapdown system in which recent advances in state-of-the-art integrated circuits of the type used in hand-held calculators, dry, two-axis, tuned-rotor rate gyros of near-inertial quality,[10-12] and off-the-shelf sun and star trackers are combined to provide an omnidirectional pointing capability with sub arc minute accuracy. There are two features of this system which make it fundamentally different from previous designs and permit it to perform in the range of much more complex ones. First, maneuvering is done solely by sequential rotations through preprogramed angles about two orthogonal control axes. This allows considerable simplification of the attitude control problem. Second, sources of pointing error inherent in all strapdown systems, i.e., biases in the gyro and electronics outputs, misalignments and nonorthogonalities of the gyro input axes, and scale factor errors are compensated for automatically. Corrections to the gyro outputs are accomplished by the use of calibration maneuvers

Received December 18, 1974; revision received April 7, 1975. The author gratefully acknowledges the support of the National Research Council for this work.

Index category: Spacecraft Attitude Dynamics and Control.

*Research Scientist, Flight Project Development Division. Formerly National Research Council Postdoctoral Fellow at the Ames Research Center. Member AIAA.

and a small, special purpose digital computer. Pointing errors have been reduced by as much as an order of magnitude compared with an uncorrected system.

System Description

A system concept employing the features described above called All Sky Pointer (ASP) has been investigated at the Ames Research Center. In operation, a spacecraft controlled by ASP establishes an inertial reference by first aligning the vehicle roll axis with the sun. The vehicle then rolls about the sun line to acquire the star Canopus with a two-axis star tracker located on its yaw axis, thus completing an inertial triad. Biases in the gyros and associated electronics, which are manifested as drift, are observed and compensated while the vehicle remains inertially fixed on the two optical references.

At the completion of the drift measurement mode, a sequence of two calibration maneuvers (see Fig. 1) is initiated. The vehicle first makes a 360° revolution about the sun line and reacquires Canopus. The second maneuver consists of three parts: a) a pitch to place Canopus in line with the yaw axis (as defined by the optical axis of the star tracker), b) a 360° yaw while controlling roll and pitch by reference to the two-axis star tracker, and c) after reacquisition of the solar yaw signal, a pitch in the opposite direction from the initial pitch motion in order to null the sun sensor pitch signal and return to the original orientation. These maneuvers permit the measurement and correction of scale factor errors in both the gyros and electronics, and of errors arising from misalignments of the gyro input axes.

The scientific instrumentation of the vehicle is aimed at targets of interest following the calibration sequence by a series of roll and yaw maneuvers through precomputed angles stored in the ASP memory. The vehicle may observe any number of targets as well as return to the sun-Canopus reference periodically in order to eliminate errors which accumulate with multiple maneuvers and residual drift.

The ASP system incorporated two nonfloated two-axis, tuned-rotor rate gyros† with their input axes oriented to form a triad nominally orthogonal and aligned with the optical axes of the sun and star trackers. The optical axis of the sun sensor defines the vehicle roll axis, while the optical axis of the star tracker, aligned precisely 90° to the sun sensor, defines the vehicle yaw axis. Gyro outputs are converted to pulses and pseudo-integrated by an up-down counter. Digitizing these signals provides the advantages of wide dynamic range, ease of integration with minimal electronic drift, and the precision afforded by digital computations.

The electronics package contains a master sequencer, analog control system electronics, and the equivalent of a four function calculator used to compute the scale factor and misalignment terms derived from the calibration maneuvers. Control torques may be supplied by gas jets, reaction wheels, CMG's, or other appropriate means.

Discussion of Error Sources

There are four primary sources of error related to the use of body-fixed rate gyros that affect the fundamental pointing precision of a strapped down system such as ASP. They are as follows.

Scale factor errors. Coffman[9] tested a number of rate gyros suitable for strapped down applications and found scale factor errors from this source alone, for a single axis maneuver of 60°, range from 50-1000 arc sec (140-3000 ppm). Additional pointing errors would result from the integration of scale factor errors.

Gyro input axis misalignment. Alignment of the gyro input axis triad is crucial to the performance of strapdown systems.

†Although two-axis tuned-rotor gyros were used in a laboratory model of ASP, any type of angular rate sensor, single or multi-axis, floated or dry, is acceptable.

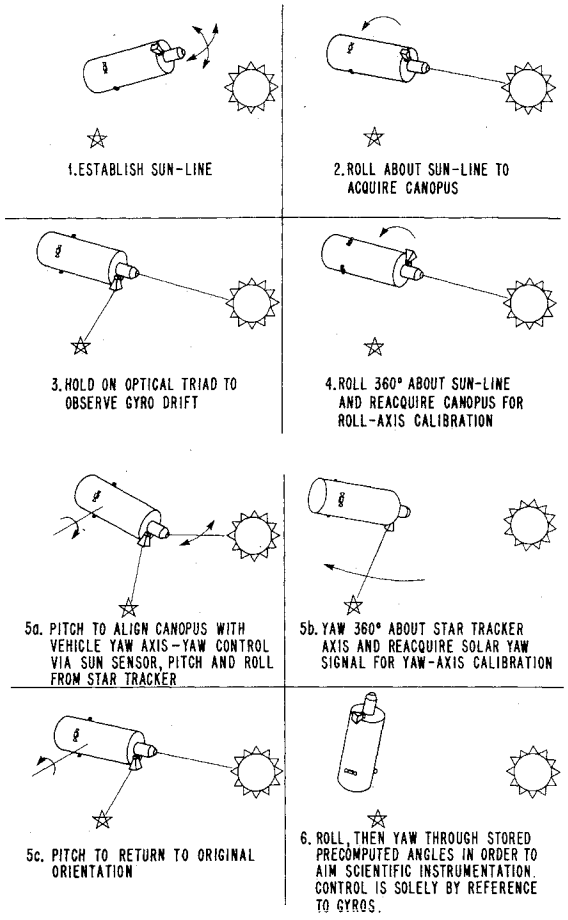

Fig. 1 All sky pointer calibration and target acquisition maneuver sequence.

Mutual nonorthogonality in the gyro input axes (typically, between 5 and 30 arc sec) results in a cross coupling effect that appears as drift during a maneuver. A more serious source of error is the misalignment between the null axis of the optical sensors (and scientific instruments) and the gyro input axes. While initial alignment may be as close as 10-20 arc sec, shifts in the electronic and mechanical null caused by structural flexing, vibration, aging, and thermal effects may increase the original error by an order of magnitude.

Bias and noise in gyro and integrator outputs. A nonzero output of the gyro-integrator pair for a zero input results in pointing errors upon completion of a maneuver as well as a continuing post-maneuver drift. Rate noise (noise in the gyro outputs) affects pointing accuracy and degrades drift performance because of the uncertainty it introduces into the integated gyro output. Feldman[11] reports rate noise components for certain gyros suitable for ASP ranging from 0.005-0.030 deg/hr.

Nonlinear effects. There are a number of higher-order effects such as inter-axis coupling in two axis gyros, nonlinear scale factor, differing positive and negative scale factor, and bias drift that adversely affect pointing performance. While this analysis does not attempt to model these effects, the system operates in a manner that minimizes errors from these sources. For example, maneuvering is done at one rate around one axis at a time in order to reduce the effects of scale factor nonlinearities and inter-axis coupling.

The optical axes of the sun and star trackers form the control axis triad. There are four properties of the optical sensor model that are critical to pointing performance: a) inter-axis alignment between the sun and star trackers, b) stability including mechanical, electronic, and optical shifts of the sensor axes, c) resolution, and c) noise equivalent angle. Knowledge of the location of the optical axes of the two sensors permits

Table 1 Performance of typical sun and star trackers

	Resolution (arc sec)	Stability (arc sec hr)	Noise equivalent angle (rms arc sec)
SPARCS			
Fine sun sensor	0.1	1	0.1
JPL			
Canopus tracker	<10	1.2	17
ITT			
Star tracker	1	0.2	0.4

them to be aligned precisely orthogonal to one another. Good stablity assures that this alignment will be maintained. The quality of the attitude control and the measurement of the gyro-related errors is also obviously dependent upon the sensor resolution and noise. Linearity and scale factor are not important since the controller is null-seeking and no absolute measurements are being performed. Table 1 lists typical sun and star tracker parameters.

Equations of Motion

Figure 2 depicts the general arrangement of the gyro input axes in an ASP-controlled vehicle. The direction cosines relating the orientation of each gyro input axis to the principal axes of inertia of the vehicle are contained in the alignment matrix A. Thus, the sensed components of the angular velocity vector ω are

$$\begin{bmatrix} \omega_{s1} \\ \omega_{s2} \\ \omega_{s3} \end{bmatrix} = \begin{bmatrix} A_{11} & A_{12} & A_{13} \\ A_{21} & A_{22} & A_{23} \\ A_{31} & A_{32} & A_{33} \end{bmatrix} \begin{bmatrix} \omega_1 \\ \omega_2 \\ \omega_3 \end{bmatrix} \tag{1}$$

When the biases and scale factors of the gyro and integrator are included, the angles measured by each of the gyros are represented by equations of the form

$$\theta_{mj} = S_{Ij} \int_0^t [S_{Gj}(\omega_{sj} + b_{Gj}) + b_{Ij}]\,d\tau \quad j = 1,2,3 \tag{2}$$

As a result of combining Eqs. (1) and (2), a set of differential equations relating the measured angles to the vehicle body rates are formed

$$\dot{\theta}_{mj} = S_{Ij}S_{Gj}(A_{j1}\omega_1 + A_{j2}\omega_2 + A_{j3}\omega_3) + S_{Ij}(S_{Gj}b_{Gj} + b_{Ij}) + \eta_j \tag{3}$$

Equation (3) indicates that the components of the alignment matrix and the gyro drift terms cannot be observed independently of the scale factors S_G and S_I. However, obtaining a measure of the apparent alignment and bias terms is all that is required to compensate for their effects. Thus A^*, the apparent-alignment matrix, has components $S_{Ij}S_{Gj}A_{jk}$.

The initial operation of the control system after establishing an inertial reference is measurement of the gyro drift (bias). The vehicle is controlled by reference to the sun and Canopus in this mode, thereby maintaining the effective body rates at zero. The gyro output is observed over a period T and the compensating bias terms are calculated at its conclusion.

If we assume that the vehicle remains stationary during the measurement period, then the bias term for each axis is

$$B_j = \frac{1}{T}\int_0^T \dot{\theta}_{mj}\,d\tau = S_{Ij}(S_{Gj}b_{Gj} + b_{Ij}) + \frac{\gamma_j}{T} \tag{4}$$

The length of the measurement period T is based on several criteria: the covariance of the gyro and integrator random noise, the period of the controller limit cycles, and the capacity of the device which stores the drift angle. The most important factor in the choice of T is the covariance of the gyro and integrator noise. Since the output of the integrator, after compensation, is

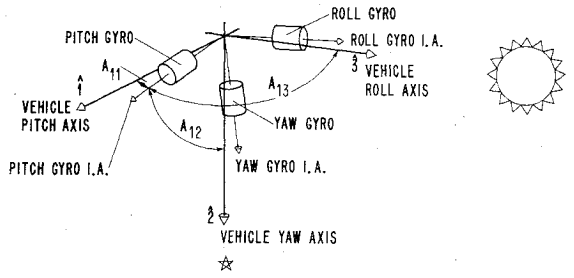

Fig. 2 Gyro input axis orientation relative to body principal axes.

$$\epsilon_j = \int_0^t [S_{Ij}(S_{Gj}b_{Gj} + b_{Ij} - B_j) + \eta_j]\,d\tau \tag{5}$$

substituting Eq. (4) into Eq. (5), the residual of the compensated drift is

$$\dot{\epsilon}_j = S_{Ij}(1 - S_{Ij})(S_{Gj}b_{Gj} + b_{Ij}) + \eta_j - S_{Ij}(\gamma_j/T) \tag{6}$$

thus, there is a deterministic and a stochastic component of residual drift characteristics of this compensation technique. The portion due to the integrator scale factor is four orders of magnitude below the values of b_G and b_I for typical values of S_I and is of little consequence. If $E\{\eta^2\} = R^2\delta(t)$, then $E\{\gamma^2/T^2\} = (R^2/T)\delta(t)$. The stochastic estimation error $S_{Ij}\gamma_j/T$ has a 1σ value of $S_I RT^{-1/2}$, or for a gyro/integrator with $E\{\eta^2\} = 0.001$ (arc sec)^2/sec^2, a value of $T = 180$ sec gives an rms error of 0.002 arc sec/sec. The other considerations may require T to be as long as 500-1000 sec, thereby further reducing the stochastic drift estimation error.

After drift compensation, and assuming the errors mentioned above are negligible, Eq. (3) becomes

$$\dot{\theta}_{mj} \doteq S_{Ij}S_{Gj}(A_{j1}\omega_1 + A_{j2}\omega_2 + A_{j2}\omega_3) + \eta_j \tag{7}$$

Measurement of the apparent misalignments are made via the calibration maneuvers and Eq. (7). The first maneuver is a 360° revolution about the roll axis (vehicle-sun line), with control provided by the sun sensor error signals. The control system, locked onto the sun in pitch and yaw, maintains $\omega_1 = \omega_2 = 0$ during the maneuver. Thus, Eq. (7) may be integrated to obtain the output of each gyro-integrator pair

$$\Theta_{Rj} = \int_0^{T_{cm}} \dot{\theta}_{mj}\,d\tau = \int_0^{T_{cm}} S_{Ij}S_{Gj}A_{j\omega}\omega_3\,d\tau + \gamma_{Rj} \tag{8}$$

Three of the 9 elements in A^* may now be calculated

$$S_{Ij}S_{Gj}A_{j3} + \frac{\gamma_{Rj}}{2\pi} = \frac{\Theta_{Rj}}{2\pi} \tag{9}$$

The $\theta_{RJ}/2\pi$ are therefore the estimates of $S_{Ij}S_{Gj}A_{j3} = A^*_{j3}$.

Similarly, the 3-part yaw calibration maneuver measures the yaw axis misalignment terms by a 360° revolution of the yaw axis. The vehicle is controlled in pitch and roll by the star tracker outputs and $\omega_1 = \omega_3 = 0$. The total angle measured by a gyro integrator pair during the maneuver is the sum of the angles measured during each segment.

$$\Theta_{yj} = \int_0^{TP1} S_{Ij}S_{Gj}A_{j1}\omega_1\,d\tau + \int_0^{T_{cm}} S_{Ij}S_{Gj}A_{j2}\omega_2\,d\tau + \int_0^{TP2} S_{Ij}S_{Gj}A_{j1}\omega_1\,d\tau + (\gamma_{yj}^{(1)} + \gamma_{yj}^{(2)} + \gamma_{yj}^{(3)})/2\pi \tag{10}$$

The result of Eq. (10) is that

$$S_{Ij}S_{Gj}A_{j2}+\frac{(\gamma_{yj}^{(1)}+\gamma_{yj}^{(2)}+\gamma_{yj}^{(3)})}{2\pi}=\frac{\Theta_{yj}}{2\pi} \tag{11}$$

since

$$S_{Ij}S_{Gj}A_{j1}\left[\int_0^{TP1}\omega_1 d\tau+\int_0^{TP2}\omega_1 d\tau\right]=0 \tag{12}$$

The only net effect of the two pitch maneuvers is a small increase in the error term due to $\gamma_{yj}^{(1)}$ and $\gamma_{yj}^{(2)}$. The magnitude of the error terms may be calculated by noting that the cov $(\gamma_j)=R^2{}_jT$ so that the 1σ value for $\gamma_j=R_j(T)^{1/2}$. The roll maneuver error is thus

$$\sigma_R=\frac{\gamma_{Rj}}{2\pi}=\frac{R_j}{2\pi}(T_{cm})^{1/2} \tag{13}$$

and for the yaw maneuver

$$\sigma_y=\frac{R_j}{2\pi}(T_{cm}^{1/2}+T_{P1}^{1/2}+T_{P2}^{1/2}) \tag{14}$$

For $E\{\eta^2\}=0.001$ (arc sec)^2/sec^2, $T_{cm}=240$ sec, $T_{P1}=T_{P2}=10$ sec, $\sigma_R=3.78\times10^{-7}$ and $\sigma_Y=5.32\times10^{-7}$. This is less than 1% of the smallest value for $S_{Ij}S_{Gj}A_j$ one would expect (i.e., for the axes which are being held fixed during a maneuver).

Elements of the apparent alignment matrix A^* obtained from Eqs. (9) and (11) may now be employed directly for compensation when the vehicle is maneuvering solely by reference to the gyros. For example, during a roll maneuver we would like

$$\begin{bmatrix}\omega_1\\ \omega_2\\ \omega_3\end{bmatrix}=\begin{bmatrix}0\\ 0\\ \omega_{3c}\end{bmatrix},\quad \begin{bmatrix}\theta_{R1}\\ \theta_{R2}\\ \theta_{R3}\end{bmatrix}=\begin{bmatrix}0\\ 0\\ \theta_{3c}\end{bmatrix} \tag{15}$$

while in fact what we have, before compensation, is

$$\begin{bmatrix}\dot\theta_{1m}\\ \dot\theta_{2m}\\ \dot\theta_{3m}\end{bmatrix}=\begin{bmatrix}0\\ 0\\ \omega_{3c}\end{bmatrix},\quad \begin{bmatrix}\theta_{1m}\\ \theta_{2m}\\ \theta_{3m}\end{bmatrix}=\begin{bmatrix}0\\ 0\\ \theta_{3c}\end{bmatrix} \tag{16}$$

In order to make $\omega_1,\ \omega_2=0$ and $\omega_3=\omega_{3c}$ (i.e., correct the scaling of ω_3) the values of the gyro outputs $\dot\theta_{m1,2,3}$ must be changed. From a physical point of view, the pitch and yaw axes must be rotated at a rate equal and opposite to the rate induced by the misaligned gyros and the control system.

The output of the roll gyro must be compensated for scale factor error so that the resultant integrated angle will be correct. If $\omega_1,\ \omega_2=0$, the output of the roll integrator during a roll maneuver [from Eq. (8) with $j=3$] is

$$\theta_{R3}=S_{G3}S_{I2}A_{33}\int_0^t(\omega_{3c}+\eta_3)d\tau \tag{17}$$

thus the appropriate correction factor is $(S_{G3}S_{I3}A_{33})^{-1}$. This is one of the quantities estimated in Eq. (9) so that

$$\hat\theta_{R3}=\theta_{R3}K_{R3},\quad K_{R3}=(2\pi/\Theta_{R3}) \tag{18}$$

Equation (7) can be used to calculate the appropriate rate at which the pitch and yaw axes must be rotated to compensate for the apparent cross coupling. Setting, $\omega_1,\ \omega_2=0$ and $\omega_3=\omega_{3c}A^*{}_{33}K_{R3}$

$$\dot\theta_{mj}=S_{Ij}S_{Gj}A_{j3}\omega_{3c}+\eta_j\quad j=1,2 \tag{19}$$

so the appropriate additive correction factors are

$$-K_{Rj}\hat\theta_{R3},\ K_{Rj}=(\Theta_{Rj}/2\pi)$$

from Eq. (9). Thus, during a roll maneuver, the output of the pitch and yaw integrators is

$$\hat\theta_{Rj}=\int_0^t[S_{Ij}S_{Gj}(A_{j1}\omega_1+A_{j2}\omega_2+A_{j3}\omega_{3c})+\eta_j]d\tau-K_{Rj}\hat\theta_{R3},\ j=1,2 \tag{20}$$

and the control system will automatically force $\omega_1,\ \omega_2=0$. That is, from Eqs. (17) and (20) it can be shown that (assuming η negligible)

$$\begin{bmatrix}A_{11}^* & A_{12}^*\\ A_{21}^* & A_{22}^*\end{bmatrix}\begin{bmatrix}\omega_1\\ \omega_2\end{bmatrix}\doteq\begin{bmatrix}0\\ 0\end{bmatrix} \tag{21}$$

and since $A_{11}^*A_{22}^*>A_{12}^*A_{21}^*$ for any real system, $\omega_1,\ \omega_2=0$.

A similar series of equations may be formulated for a gyro-controlled yaw maneuver. In this case

$$\hat\theta_{y2}=\theta_{y2}K_{y2},\quad K_{y2}=(2\pi/\Theta_{y2})$$

and

$$\hat\theta_{yj}=\int_0^t[S_{Ij}S_{Gj}(A_{j1}\omega_1+A_{j2}\omega_2+A_{j3}\omega_{3c})+\eta_j]d\tau-K_{yj}\hat\theta_{y2},$$

$$K_{yj}=\frac{\Theta_{yj}}{2\pi}\quad j=1,3$$

$\omega_1,\ \omega_3=0$ by an argument identical to the previous case.

Mechanization

Figure 3 illustrates the relationships between the ASP components. A block diagram of the system is shown in Fig. 4. Note that in addition to the simplification of the gyro drift measurement discussed in Eqs. (5) and (6), it has been assumed that the control system, operating in a low-disturbance torque environment, will maintain the vehicle rate and position errors nearly at zero when controlling from the optical sensors. This approximation eliminates the necessity to correct the gyro and integrator outputs for position and rate offsets but does introduce small errors into the measurement of drift and into the correction terms K_{Rj}, K_{Yj}.

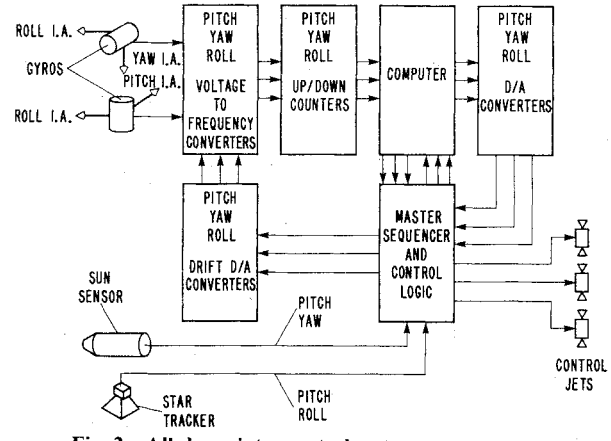

Fig. 3 All sky pointer control system components.

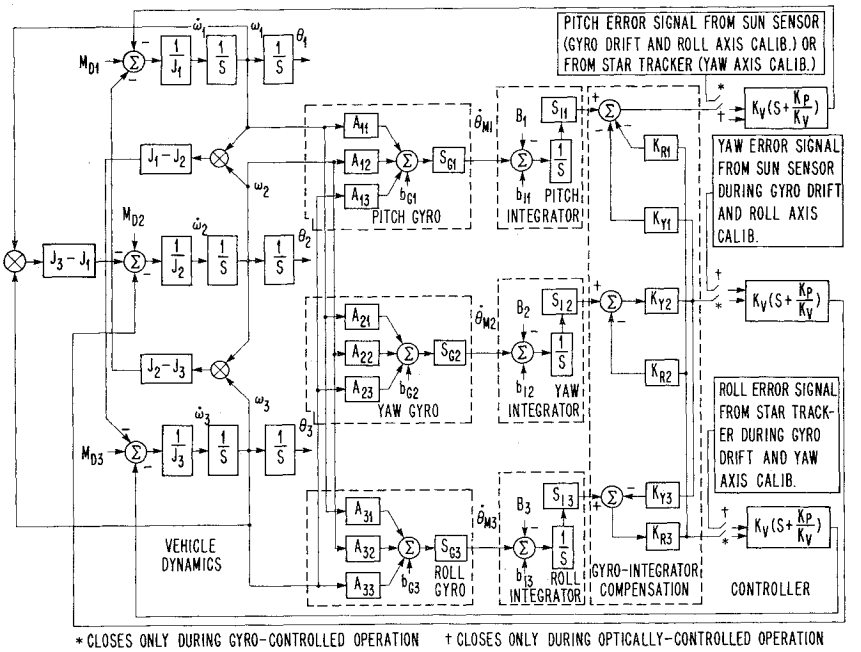

Fig. 4 Compensated gyro control loop block diagram.

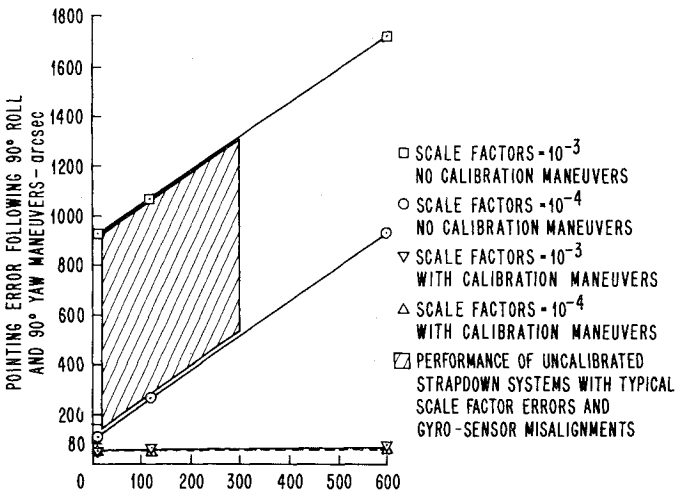

Fig. 5 A_{ij} (degree of gyro misalignment) arc sec.

Simulation Results

A three-axis digital computer simulation was developed to evaluate the performance of a hypothetical vehicle controlled by ASP and compare the results with the simulated operation of a strapdown control system not utilizing calibration maneuvers. Included in the model were nonlinearities associated with the thrusters and optical sensors, and the effects of quantization errors resulting from the conversion of the analog gyro outputs to pulses. The sun and star trackers were assumed to be aligned with principal axes of inertia. The pointing error, as well as the orientation of the vehicle relative to the simulated sun and star, was calculated by computation of the direction cosines. Two values for scale factor error, 10^{-4} and 10^{-3}, were employed while the degree of misalignment and nonorthogonality of the gyro input axes was varied from 10-600 arc sec. The sun and star are located so that the premaneuver orientation is that shown in Fig. 2.

Figure 5 is a plot of the pointing error (defined as the angle between the vehicle roll axis and a vector in the $\hat{2}$ direction of Fig. 2) following 90° roll and yaw maneuvers vs the degree of gyro misalignment. The results indicate that even with the minimum scale factor error measured by Coffman and only 10 arc sec of misalignment, the uncompensated pointing error is nearly 2-½ arc min while the error in a vehicle controlled by ASP is below 1 arc min. Any increase in gyro misalignment sharply degrades the performance of the uncalibrated system. In contrast, only a gradual increase in the pointing error of the ASP-controlled vehicle is experienced providing generally acceptable pointing error with as much as 5 arc min of misalignment.

An additional simulation of the ASP gyro drift compensation loop was performed utilizing a Teledyne Systems Co. SDG-2 two-axis tuned rotor gyro. Sinkiewicz, et al.[11] measured a similar unit to have an average uncorrected drift of approximately 1 arc sec/sec with an rms drift noise (R) of 0.02 arc sec/sec. Utilizing the drift compensation scheme described earlier, it was possible to obtain residual drift rates of less than 0.006 arc sec/sec for periods as long as 20 min when the measurements were made during quiescent conditions. The measurement period [T in Eq. (4)] was only 40 sec because of limitations in the hardware. Equation (6) indicates that a larger value of T could lead to improved performance.

Conclusions

Pointing errors in a maneuvering strapped-down attitude reference system arising from gyro-optical sensor misalignments, gyro input axis nonorthogonality, gyro-integrator scale factor errors, and biases in the gyros and integrators will be unacceptably large even with the use of the most advanced (and expensive) components and precise alignment techniques, unless compensated for in some way. A straightforward method of measuring these sources of error and compensating for them has been described in this paper. The attitude control system is mechanized utilizing relatively inexpensive off-the-shelf components and employs calibration maneuvers and sequential single-axis rotations to obtain as much of a factor of 10 reduction in pointing error when compared with an uncompensated system. Sub arc minute absolute pointing errors were achieved for operation in the forward hemisphere.

References

[1] Greeb, M.E. and Shrewsbury, D.J., "Stellar Tracking Rocket Attitude Positioning (STRAP) Systems," *Proceedings of the AIAA 2nd Sounding Rocket Vehicle Technology Conference,* Williamsburg, Va., 1970.

[2] Murphy, James P. and Lorell, Kenneth R., "The AIROSCOPE Pointing and Stabilization System," *Proceedings of the Balloon-*

Borne Astronomy Technology Conference, Ames Research Center, NASA, 1974, pp. 4.6-1-4.6-28.

[3]Remondiere, A., "The Attitude Control System 'CASSIOPEE'," *Proceedings of the AIAA 2nd Sounding Rocket Vehicle Technology Conference,* Williamsburg, Va., 1970.

[4]Van Otterloo, P., "Attitude Control for the Netherlands Astronomical Satellite (ANS)," *Phillips Technical Review,* Vol. 33, Sept. 1973, pp. 162-176.

[5]desJardins, R., "MESS (Misalignment Estimation Software System) For In-Flight Alignment and Calibration of Spacecraft Attitude Sensors," X-514-71-232, July 1971, Goddard Space Flight Center, Greenbelt, Md.

[6]Meier, J.W. and Jenkins, C.A., "Attitude Control Systems for Sounding Rockets," *Proceedings of the AIAA 2nd Sounding Rocket Vehicle Technology Conference,* Williamsburg, Va.

[7]Quasius, G.R., "Strapdown Inertial Guidance," *Space/Aeronautics,* Aug. 1963, pp. 89-94.

[8]Davis, W. R. and Miller, J. A., "SPARS—A Completely Strapdown Concept for Precise Determination of Satellite Vehicle Attitude," *Proceedings of the Symposium on Spacecraft Attitude Determination,* Vol. 1, 1969, pp. 279-291.

[9]Coffman, V. D., "On-Line Estimation of Parameters Using Experimentally Developed Gyro Models, and Other Applications," Ph.D. dissertation, Dec. 1973, Department of Aero and Astronautics, Stanford University, Stanford, Calif.

[10]Craig, R.J.G., "Theory of Operation of an Elastically Supported, Tuned Gyroscope," *IEEE Transactions on Aerospace and Electronic Systems,* Vol. AES-8, No. 3, 1972, pp. 280-288.

[11]Howe, E. W. and Savet, P. H., "The Dynamically Tuned Free Rotor Gyro," *Control Engineering,* July 1964, pp. 67-72.

[12]Sinkiewicz, J.S., Feldman, J. and Lory, C.B., "Evaluation of Selected Strapdown Inerial Instruments and Pulse Torque Loops," R-826 Final Report, Vol. I, July 1974, The Charles Stark Draper Laboratory, Inc., Cambridge, Mass.